HIGH THERMO-MECHANICAL FATIGUE AND DROP SHOCK RESISTANT ALLOYS FOR BALL-GRID ARRAY PACKAGE APPLICATIONS

Morgana Ribas, Ph.D., Suresh Telu, Ph.D., Prathap Augustine, Raghu R. Rangaraju, Anil Kumar, Divya Kosuri, Pritha Choudhury, Ph.D., Siuli Sarkar, Ph.D.
Alpha Assembly Solutions
Bangalore, KA, India
morgana.ribas@alphaassembly.com

Rommel T. Bumagat, Garian Lim
Alpha Advanced Materials
14 Joo Koon Crescent, Singapore
garian.lim@alphaassembly.com

Martin Sobczak
Alpha Advanced Materials
Suwanee, GA, USA

ABSTRACT
High-Ag, low-Ag, high-Ag plus additives: Which alloy fits best certain application? Here we present a comprehensive report on the thermal and mechanical reliability of alloys ranging from 0.3 to 3.8% Ag, with and without presence of additives such as Bi, Ni and Sb. CTBGA packages with 84 I/Os were assembled using Sn-1Ag-0.5Cu, Sn-0.3Ag-0.7Cu-X, Sn-1.2Ag-0.5Cu-0.05Ni, Sn-3Ag-0.5Cu, Sn-3.8Ag-0.7Cu-Sb-Bi-X and Sn-3.8Ag-0.8Cu-Bi-X spheres. Test vehicle assembly used Sn-3Ag-0.5Cu solder paste for all alloys, except for Sn-3.8Ag-0.8Cu-Bi-X BGAs, which were evaluated with both Sn-3Ag-0.5Cu and Sn-3.8Ag-0.8Cu-Bi-X solder pastes. Single ball shear, drop shock and thermal cycling were used to evaluate these alloys performance for BGA packages applications. Our results expand the perspective over the usual belief that high-Ag Sn-Ag-Cu alloys result in better thermal cycling and lower drop shock performance than when using low-Ag alloys.

Alloying additions can be used to improve single ball shear, drop shock and thermal cycling properties. In order to obtain maximum performance and cost benefit, solder alloys need to be paired to the correct application. Based on the results shown, we recommend: i) Sn-0.3Ag-0.7Cu-X for applications that require maximum drop shock and reasonable thermal cycling performance. ii) Sn-3Ag-0.5Cu for applications requiring good drop shock and thermal cycling properties. iii) Sn-3.8Ag-0.8Cu-Bi-X for applications that require higher shear strength, drop shock and thermal cycling, including automotive under the hood, high efficiency LEDs and semiconductor packaging.

Key words: Ball-grid array packages, lead-free, solder alloys, thermal cycling, drop shock

INTRODUCTION
Lead-free alloys Sn-3Ag-0.5Cu and Sn-4Ag-0.5Cu are popular choices that have been commonly used since the electronics industry transitioned to lead-free solders [1-3]. They are particularly known to have thermal cycling properties superior to eutectic Sn-Pb [4-5]. Unfortunately, these high silver Sn-Ag-Cu alloys do not reproduce Sn-Pb mechanical reliability performance. As devices complexity increased and they became smaller and more portable, there was a need to improve mechanical reliability of Sn-Ag-Cu alloys. One of the solutions was to reduce silver content in Sn-Ag-Cu alloys, generally resulting in improved drop shock resistance [6-7]. Alloys with silver content below 1 wt.% became popular choices as they were better suited for portable electronics. In addition to that, lowering silver content reduces exposure to its market price oscillations, resulting in more stable soldering materials costs.

However, certain applications still required alloys with higher thermal reliability than Sn-3Ag-0.5Cu/Sn-4Ag-0.5Cu alloys [8]. Therefore, high silver Sn-Ag-Cu alloys with performance additives such as Sb, Bi and Ni were introduced and, especially recommended, for automotive and energy technology applications [9-12]. In the case of semiconductors applications, there is limited information on how these various alloys fare against each other. In addition to that, practical reasons could lead electronics manufacturers to continue using Sn-3Ag-0.5Cu solder paste, despite switching the solder alloy in the components.

In the work presented here, for the first time we present a comprehensive investigation of thermo-mechanical reliability of mixed lead-free Sn-Ag-Cu solder alloys. The six alloys evaluated for ball-grid array (BGA) applications include alloys with Ag content from 0.3 to 3.8%, and other

alloying additions including Ni, Bi and Sb. In order to obtain maximum performance and cost benefit, solder alloys need to be paired to the correct application. Here we evaluate these alloys single ball shear, high temperature storage, thermal cycling, and drop performance, and conclude on their suitability for various thermo-mechanical reliability requirements.

EXPERIMENTAL DETAILS

Total of seven sphere-solder paste combinations were chosen for this study, as shown in Table 1. These include three low silver and three high silver alloys. Sn-1.2Ag-0.5Cu-0.05Ni is also known as SAC125N, Sn-0.3Ag-0.7Cu-X is called SACX Plus 0307, Sn-3.8Ag-0.7Cu-Sb-Bi-X is also known as Innolot or Maxrel, and Sn-3.8Ag-0.8Cu-Bi-X is called Maxrel Plus. Sn-0.3Ag-0.7Cu-X contains proprietary additives to enhance its mechanical reliability, whereas Sn-3.8Ag-0.7Cu-Sb-Bi-X is known to have improved thermal cycling performance. Sn-3.8Ag-0.8Cu-Bi-X is a recently introduced ultra-high reliability alloy. All solder pastes were prepared using a no-clean rosin solder paste flux. CTBGA84 with Ni-Au finish 0.225 mm pad size were assembled using 12 mil spheres of each of the alloys.

Table 1. Test matrix of sphere-solder paste alloy combinations

ID	Sphere	Solder Paste
AA	Sn-3Ag-0.5Cu	Sn-3Ag-0.5Cu
BA	Sn-1Ag-0.5Cu	Sn-3Ag-0.5Cu
CA	Sn-0.3Ag-0.7Cu-X	Sn-3Ag-0.5Cu
DA	Sn-1.2Ag-0.5Cu-0.05Ni	Sn-3Ag-0.5Cu
EA	Sn-3.8Ag-0.7Cu-Sb-Bi-X	Sn-3Ag-0.5Cu
FA	Sn-3.8Ag-0.8Cu-Bi-X	Sn-3Ag-0.5Cu
FB	Sn-3.8Ag-0.8Cu-Bi-X	Sn-3.8Ag-0.8Cu-Bi-X

Single Ball Shear

Single ball shear test was conducted in a Condor Sigma bond tester (Figure 1). From the two outermost rows of the CTBGA84 (Figure 1 inset), each sphere is sheared at 700 µm/s test speed. A total of five BGAs were tested and the average single ball shear strength of each alloy was computed.

Figure 1. Condor Sigma bond tester. CTBGA84 (inset)

Drop Shock

The same test vehicle was used for thermal cycling and drop shock evaluation (Figure 2). This test vehicle is a copper OSP, 77 x 132 mm, non-solder mask defined PCB, with 15 CTBGA84 components per board. A Lansmont M23 shock machine, shown in Figure 3 (left), is used for performing the drop tests of our customized test vehicle. By adjusting the drop height and the strike surface it is possible to achieve JEDEC's recommended service condition B (1500Gs, 0.5 msec duration and half-sine pulse), which is monitored as shown in Figure 3 (right).

The electrical continuity of each component is monitored during each drop using an event detector. Each of the CTBGA84 units on the drop shock test vehicle was tested till failure as per JESD22-B111 standard. Failures were recorded once a first discontinuity is followed by three others, within five subsequent drops. Weibull curves were built for evaluating the probability distribution of the failures over a period of time.

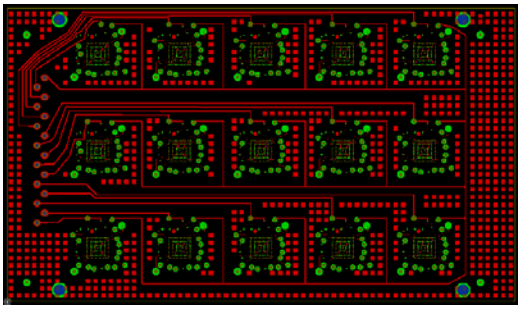

Figure 2. Test vehicle used for thermal cycling and drop shock tests

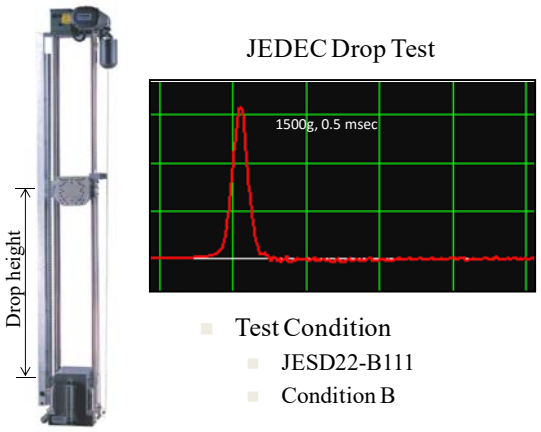

Figure 3. Lansmont drop shock testing machine (left) and half-sine shock pulse curve (right)

Thermal Cycling

Thermal cycling tests were carried out in an air-to-air Espec chamber (model TSA-101S), Figure 4 (top). Thermal cycling profile followed JEDEC condition G of the JESD22-A104 standard, from -40°C to 125°C, with 10 min dwell at the extreme temperatures, as shown in Figure 4 (bottom). The components were electrically monitored for discontinuities/increase in contact resistance for a total of 4,000 thermal cycles using a data logger.

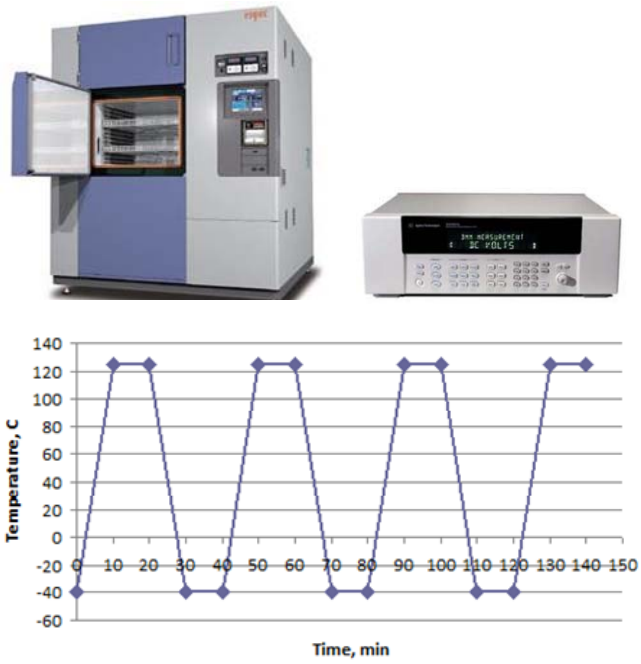

Figure 4. Equipment (top) and thermal profile (bottom) used in the thermal cycling test

High Temperature Storage

The effect of high temperature storage on the alloy microstructure and intermetallics were also evaluated. Test vehicles were assembled with CTBGA84 as per sphere-solder paste combinations shown in Table 1. Samples were uniformly maintained at 150°C for up to 1000 hours. Sampling was done at 250, 500, 750 and 1000 hours intervals.

Intermetallics Analysis

The effect of thermal cycling and high temperature storage on the solder joints of the new alloys was also evaluated. Cross-sections of each assembly were investigated using a scanning electron microscope (SEM) in order to assess the solder joint integrity of the respective sphere-solder paste combinations. In addition to that, the interfacial intermetallics thickness was measured, on both PCB and component sides.

RESULTS AND DISCUSSION

Results of single ball shear strength are shown in Figure 5. Sn-3.8Ag-0.7Cu-Sb-Bi-X and Sn-3.8Ag-0.8Cu-Bi-X average shear strength is 73% higher than Sn-3Ag-0.5Cu and 100-114% higher than the low-Ag alloys. Sn-3.8Ag-0.7Cu-Sb-Bi-X and Sn-3.8Ag-0.8Cu-Bi-X have a little higher Ag content than Sn-3Ag-0.5Cu, so Ag addition alone is not responsible for their higher shear strength. Both Sn-3.8Ag-0.7Cu-Sb-Bi-X and Sn-3.8Ag-0.8Cu-Bi-X have Bi addition, which increases the alloy strength through solid solution. In the case of Sn-3.8Ag-0.7Cu-Sb-Bi-X, Sb addition also contributes to its solid solution strengthening. Sn-3.8Ag-0.8Cu-Bi-X has other additives that bring its strength to the same level of Sn-3.8Ag-0.7Cu-Sb-Bi-X, despite being a Sb-free alloy. There is very little difference in shear strength between the alloys from 0.3 to 1.25 wt.% Ag. Therefore, it is fair to conclude that Ag addition has only a minor effect on the single ball shear strength of these alloys.

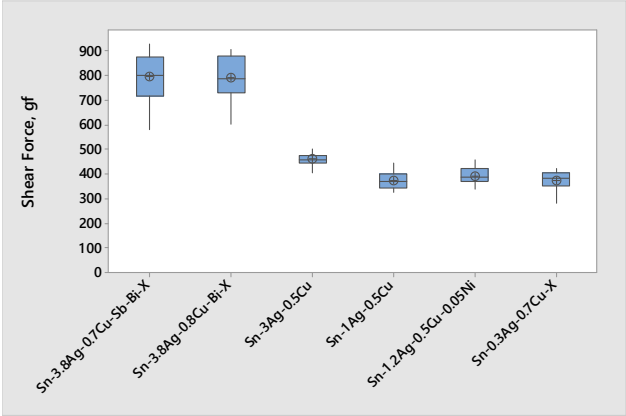

Figure 5. Single ball shear strength

Single ball shear strength was found to be a poor indication of drop shock performance of these alloys, which is shown in Figure 6. For example, Sn-3.8Ag-0.7Cu-Sb-Bi-X and Sn-1.2Ag-0.5Cu-0.05Ni BGAs resulted in the worst drop shock characteristic life. Sn-1Ag-0.5Cu and Sn-3Ag-0.5Cu have similar drop shock performance, but use of Sn-3.8Ag-0.8Cu-Bi-X spheres increases drop shock characteristic life in 43%. Sn-0.3Ag-0.7Cu-X and Sn-3.8Ag-0.8Cu-Bi-X showed the best drop shock performance among the alloys tested. The superior performance of Sn-0.3Ag-0.7Cu-X and

Sn-3.8Ag-0.8Cu-Bi-X does not come as a surprise given the fact that these alloys were specifically developed for maximized thermo-mechanical performance. Both of these alloys have additives that control atomic diffusion during interfacial intermetallics formation. Although Sn-3.8Ag-0.8Cu-Bi-X is a high-Ag alloy, its additives confine Ag_3Sn mostly to within the eutectic phase.

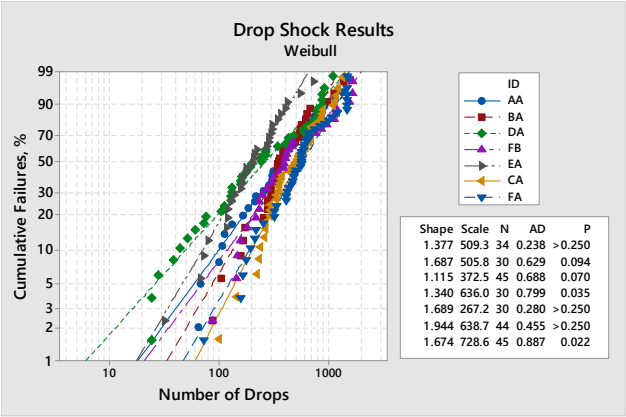

Figure 6. Drop shock performance of sphere-solder paste combinations

Thermal cycling results are summarized in Table 2. Sn-1Ag-0.5Cu has the poorest thermal cycling performance, with 100% BGA electrical failures before 3000 cycles. By 3500 thermal cycles, Sn-0.3Ag-0.7Cu-X, Sn-1.2Ag-0.5Cu-0.05Ni and Sn-3Ag-0.5Cu BGAs also have also showed 100% failures. At the end of the test completion (4000 cycles), 9-20% Sn-3.8Ag-0.8Cu-Bi-X BGAs had failed, whereas 37.8% of Sn-3.8Ag-0.7Cu-Sb-Bi-X BGAs failed. The Weibull curves representing these results are shown in Figure 7.

Sn-0.3Ag-0.7Cu-X thermal cycling characteristic life is 11% higher than Sn-1Ag-0.5Cu. Thus, despite its lower Ag content, Sn-0.3Ag-0.7Cu-X thermal cycling is higher than what is expected due to its alloying additions. Sn-1.2Ag-0.5Cu-0.05Ni, which has four times more Ag than Sn-0.3Ag-0.7Cu-X is 24% higher. Perhaps the most surprising results is that Sn-3Ag-0.5Cu thermal cycling was just 3% higher than Sn-1.2Ag-0.5Cu-0.05Ni. Sn-3.8Ag-0.7Cu-Sb-Bi-X, which is known for its high thermal fatigue properties, showed 68% higher performance than Sn-3Ag-0.5Cu. Both sets using Sn-3.8Ag-0.8Cu-Bi-X spheres showed excellent thermal cycling performance, with considerably less cumulative failures than Sn-3.8Ag-0.7Cu-Sb-Bi-X. However, due to the small number of failures, their Weibull curves are less accurate in describing their behaviour.

Table 2. Cumulative failures after thermal cycling test

ID	Cumulative Failures (%)							
	0- 500 TC	0- 1000 TC	0- 1500 TC	0- 2000 TC	0-2500 TC	0- 3000 TC	0- 3500 TC	0-4000 TC
BA	0	0	24.4	51.1	86.7	100	100	100
CA	0	0	4.5	40.1	79.5	97.7	100	100
DA	0	0	0	2.2	26.7	75.6	100	100
AA	0	0	0	2.2	20	68.9	100	100
EA	0	0	0	2.2	2.2	11.1	24.4	37.8
FB	0	0	0	0	2.2	4.4	17.8	20
FA	0	0	0	0	0	0	4.5	9

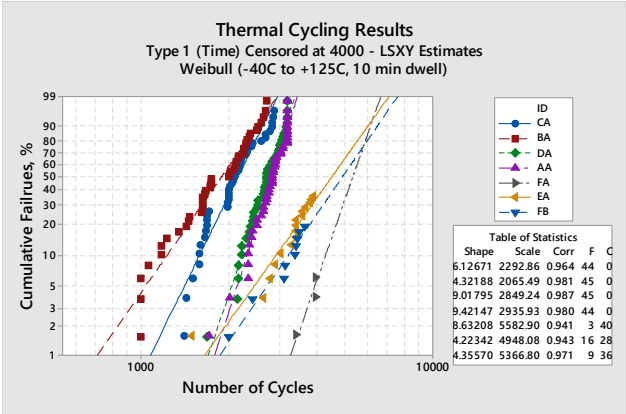

Figure 7. Weibull curves of thermal cycling test results

Various solder joints were analysed through cross-sections after 4000 cycles. This analysis confirmed the electrical failures and depict the solder joint performance after such extensive thermal cycling test. Images representing typical failure modes of these solder joints are shown in Figure 8. The low-Ag spheres showed extensive cracks (Figure 8 a-c), which sometimes run across between PCB and component, whereas Sn-3Ag-0.5Cu showed less extensive cracks (Figure 8 d). Unlike these alloys, the combination of high-Ag and additives of Sn-3.8Ag-0.7Cu-Sb-Bi-X (Figure 8 e) and Sn-3.8Ag-0.8Cu-Bi-X (Figure f-g) resulted in only minor cracks after 4000 thermal cycles.

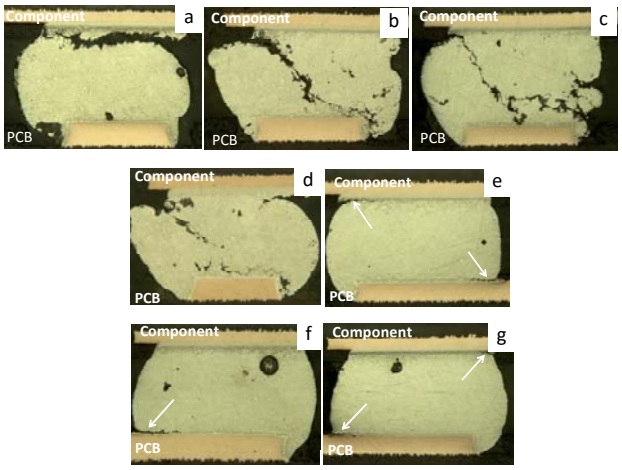

Figure 8. Cross-sections after 4,000 thermal cycles. a) Sn-1Ag-0.5Cu, b) Sn-1.2Ag-0.5Cu-0.05Ni, c) Sn-0.3Ag-0.7Cu-X, d) Sn-3Ag-0.5Cu, e) Sn-3.8Ag-0.7Cu-Sb-Bi-X, f) Sn-3.8Ag-0.8Cu-Bi-X (FA), and g) Sn-3.8Ag-0.8Cu-Bi-X (FB)

The effect of high temperature storage on intermetallics thickness was evaluated on both component and PCB sides. Table 3 shows the intermetallics thickness on the component-solder interface, i.e., solder on Ni-Au finish, whereas Table 4 shows the intermetallics thickness on solder-PCB interface, i.e., solder on OSP finish. Figure 9 show the initial intermetallics and microstructure appearance on both interfaces.

Table 3. Intermetallics thickness after high temperature storage (in hours) measured on component-solder interface

Alloy	0	100	250	500	1000
Sn-0.3Ag-0.7Cu-X	2.29	2.28	2.48	2.79	3.46
Sn-1Ag-0.5Cu	2.48	2.71	3.14	3.38	4.08
Sn-1.2Ag-0.5Cu-0.05Ni	2.37	2.28	2.58	2.94	3.50
Sn-3Ag-0.5Cu	2.31	2.56	2.56	2.63	2.80
Sn-3.8Ag-0.7Cu-Sb-Bi-X	1.65	2.04	2.16	2.32	2.85
Sn-3.8Ag-0.8Cu-Bi-X (FA)	2.25	2.35	3.07	3.47	3.75
Sn-3.8Ag-0.8Cu-Bi-X (FB)	2.28	2.35	2.54	2.86	3.43

Initial intermetallics thickness on the component-solder interface is between 2.25 and 2.48 µm, except for Sn-3.8Ag-0.7Cu-Sb-Bi-X, which was 1.65 µm. After 1000 hrs, Sn-3Ag-0.5Cu and Sn-3.8Ag-0.7Cu-Sb-Bi-X showed thinner thickness, around 2.80 µm. The intermetallics of the other alloys was between 3.43 and 4.08 µm. Sn-3Ag-0.5Cu showed the lowest growth in intermetallics thickness due to high temperature storage (21%), whereas Sn-3.8Ag-0.7Cu-Sb-Bi-X had the highest growth (73%).

On the solder-PCB interface, Sn-3.8Ag-0.7Cu-Sb-Bi-X initial intermetallics thickness was also the thinnest (1.61 µm), followed by Sn-0.3Ag-0.7Cu-X (1.77 µm). Other alloys were between 2.19 and 2.59 µm. Sn-3.8Ag-0.7Cu-Sb-Bi-X, Sn-3.8Ag-0.8Cu-Bi-X (FA), and Sn-0.3Ag-0.7Cu-X intermetallics thickness more than double after 1000 hrs, whereas Sn-3Ag-0.5Cu, Sn-1.2Ag-0.5Cu-0.05Ni and Sn-3.8Ag-0.8Cu-Bi-X (FB) showed lower growth (45-65%).

Table 4. Intermetallics thickness after high temperature storage (in hours) measured on solder-PCB interface

Alloy	0	100	250	500	1000
Sn-0.3Ag-0.7Cu-X	1.77	2.05	2.91	3.38	3.99
Sn-1Ag-0.5Cu	2.19	2.21	2.83	3.28	4.04
Sn-1.2Ag-0.5Cu-0.05Ni	2.30	2.18	2.75	3.09	3.40
Sn-3Ag-0.5Cu	2.48	2.57	2.84	3.26	3.59
Sn-3.8Ag-0.7Cu-Sb-Bi-X	1.61	2.10	2.60	2.72	3.49
Sn-3.8Ag-0.8Cu-Bi-X (FA)	2.17	2.45	3.65	4.07	4.93
Sn-3.8Ag-0.8Cu-Bi-X (FB)	2.59	2.47	3.09	3.59	4.28

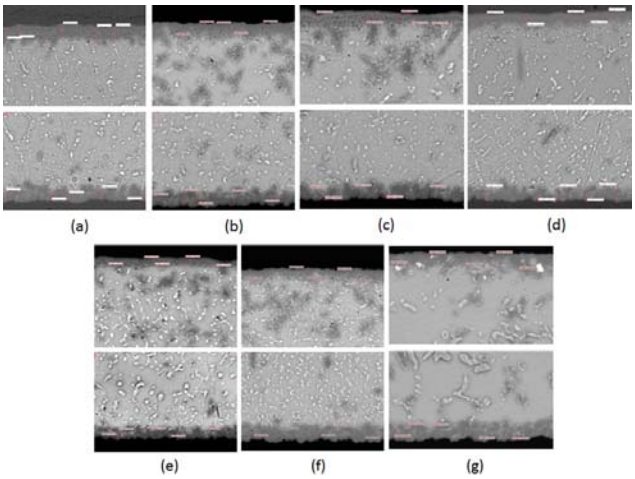

Figure 9. Intermetallics and microstructure for: . a) Sn-1Ag-0.5Cu, b) Sn-1.2Ag-0.5Cu-0.05Ni, c) Sn-0.3Ag-0.7Cu-X, d) Sn-3Ag-0.5Cu, e) Sn-3.8Ag-0.7Cu-Sb-Bi-X, f) Sn-3.8Ag-0.8Cu-Bi-X (FA), and g) Sn-3.8Ag-0.8Cu-Bi-X (FB). PCB at the bottom.

CONCLUSIONS

We have shown here a little broader perspective over the usual belief that higher drop shock performance is achieved using lower-Ag Sn-Ag-Cu alloys, whereas high thermal

cycling results from higher-Ag content. By performing a very comprehensive study of six alloys with various degrees of Ag content and additives, we were able to draw the following conclusions:
Given these results, we conclude that: i) Bi, Sb and other alloying additions can significantly increase single ball shear strength, ii) Sn-0.3Ag-0.7Cu-X and Sn-3.8Ag-0.8Cu-Bi-X presented the highest drop shock performance, which is attributed to additives that control atomic diffusion at the substrate interface and in the bulk solder, iii) Increasing Ag in the solder alloy (e.g., Sn-3Ag-0.5Cu) improves thermal cycling, but its performance can be further improved by combining higher-Ag content and performance additives as shown for Sn-3.8Ag-0.7Cu-Sb-Bi-X and Sn-3.8Ag-0.8Cu-Bi-X alloys.

In order to obtain maximum performance and cost benefit, solder alloys need to be paired to the correct application. Among the low-Ag alloys, Sn-0.3Ag-0.7Cu-X (i.e., SACX Plus 0307) provides the best drop shock and thermal cycling performance. Sn-3Ag-0.5Cu provides good drop shock and thermal cycling properties. For applications that require higher thermal reliability performance, including shear strength and thermal cycling, Sn-3.8Ag-0.7Cu-Sb-Bi-X (i.e., Innolot or Maxrel) and Sn-3.8Ag-0.8Cu-Bi-X (i.e., Maxrel Plus) are recommended. In addition to that, Sn-3.8Ag-0.8Cu-Bi-X also delivers excellent drop shock (and vibration) performance, and is particularly recommended for applications such as automotive under the hood, high efficiency LEDs and semiconductor packaging.

REFERENCES

1. “Round Robin testing and Analysis of Lead Free Solder Pastes with Alloys of Tin, Silver, Copper” – Final Report, IPC Solder Products Value Council.

2. Anderson, I.E., “Development of Sn-Ag-Cu and Sn-Ag-Cu-X alloys for Pb-free electronic solder applications”. *J. Mater. Sci.: Mater. Electron.*, 18 (2007) pp.55-76.

3. Handwerker, C., Kattner, U., and Moon, K.W., “Fundamental Properties of Pb-Free Solder Alloys”. Lead-Free Soldering, Ed. J. Bath, Springer, 2007.

4. Henshall, G. et al., “iNEMI Pb-Free Alloy Alternatives Project Report: State of the Industry”. *J. SMT*, 21 (2008), pp.11-23.

5. Henshall, G. et al., “Low-Silver BGA Assembly Phase II – Reliability Assessment Sixth Report: Thermal Cycling Results for Unmixed Joints”. Proc. of SMTA International, Orlando, October, 2010.

6. Pandher, R. et al., “Drop Shock Reliability of Lead-Free Alloys - Effect of Micro-Additives”. Proc. 57th Electronic Components and Technology Conf., Reno, NV, May. 2007, pp. 669-676.

7. Pandher, R. and Healey, R., “Reliability of Pb-free Solder Alloys in Demanding BGA and CSP Applications”. Proc. 58th Electronic Components and Technology Conf., Orlando, FL, May. 2008, pp. 2018-2023.

8. Hillman, C., “Reality of New, High Reliability Solders”. DfR Solutions Monthly Webinars, February, 2016.

9. Steen, H. and Toleno, B., “Development of a Lead-Free Alloy for High-Reliability, High-Temperature Applications”. Proc. of IPC APEX EXPO.

10. Choudhury, P. et. al., “New lead-free alloy for high reliability, high operating temperature conditions,” SMTA ICSR (Soldering and Reliability) Conference Proceedings, Toronto. May (2014).

11. Choudhury, P. et. al., “Development of Lead-Free Alloys with Ultra-High Thermo-Mechanical Reliability”, Proc. of SMTA International, Chicago, September, 2015.

12. Bent, W. et al., “Low Voiding, High Reliability Solder Paste for Automotive, LED and Other Demanding Applications”. Proc. of SMTA International, Chicago, September, 2015.